Intercellular Adhesion Molecule-1–Deficient Mice Are Resistant Against Renal Injury After Induction of Diabetes

Shinichi Okada, Kenichi Shikata, Mitsuhiro Matsuda, Daisuke Ogawa, Hitomi Usui, Yuichi Kido, Ryo Nagase, Jun Wada, Yasushi Shikata, and Hirofumi Makino

Diabetic nephropathy is a leading cause of end-stage renal failure. Several mechanisms, including activation of protein kinase C, advanced glycation end products, and overexpression of transforming growth factor (TGF)-β, are believed to be involved in the pathogenesis of diabetic nephropathy. However, the significance of inflammatory processes in the pathogenesis of diabetic microvascular complications is poorly understood. Accumulation of macrophages and overexpression of leukocyte adhesion molecules and chemokines are prominent in diabetic human kidney tissues. We previously demonstrated that intercellular adhesion molecule (ICAM)-1 mediates macrophage infiltration into the diabetic kidney. In the present study, to investigate the role of ICAM-1 in diabetic nephropathy, we induced diabetes in ICAM-1–deficient (*ICAM-1*$^{-/-}$) mice and *ICAM-1*$^{+/+}$ mice with streptozotocin and examined the renal pathology over a period of 6 months. The infiltration of macrophages was markedly suppressed in diabetic *ICAM-1*$^{-/-}$ mice compared with that of *ICAM-1*$^{+/+}$ mice. Urinary albumin excretion, glomerular hypertrophy, and mesangial matrix expansion were significantly lower in diabetic *ICAM-1*$^{-/-}$ mice than in diabetic *ICAM-1*$^{+/+}$ mice. Moreover, expressions of TGF-β and type IV collagen in glomeruli were also suppressed in diabetic *ICAM-1*$^{-/-}$ mice. These results suggest that ICAM-1 is critically involved in the pathogenesis of diabetic nephropathy. *Diabetes* 52:2586–2593, 2003

Diabetic nephropathy is a major complication of diabetes and a leading cause of end-stage renal failure in developed countries. Several mechanisms have been postulated for the development of diabetic nephropathy. Hyperglycemia accelerates the accumulation of diacylglycerol, resulting in activation of protein kinase C, which enhances the expression of transforming growth factor (TGF)-β and overproduction of the extracellular matrix (ECM) by mesangial cells (1). Advanced glycation end products (AGEs) can also stimulate mesangial cells to produce ECM, such as type IV collagen (2,3). On the other hand, hemodynamic changes in diabetic glomeruli are also an important cause of glomerular injury in diabetic patients.

Infiltration of macrophages in the glomeruli and interstitium is one of the characteristic features of diabetic nephropathy, in addition to ECM expansion and interstitial fibrosis (4,5). Furuta et al. (4) reported that the number of macrophages in the glomeruli was significantly higher in the moderate stage of diabetic glomerulosclerosis compared with the advanced stage in human renal biopsy specimens, suggesting the pathological role of macrophages in the development of diabetic nephropathy.

Leukocyte infiltration into inflammatory or atherosclerotic lesions is mediated by sequential engagement of cell adhesion molecules and chemokines. Leukocyte influx begins with leukocyte rolling and firm attachment (sticking) to the endothelium, followed by transmigration across the endothelial surface. Intercellular adhesion molecule (ICAM)-1, a cell-surface protein with five immunoglobulin-like domains, is one of the major molecules involved in promoting leukocyte firm attachment to the endothelium and transmigration through its expression on the vascular endothelium and binding to β_2 leukocyte integrins (6). In the kidney, ICAM-1 is upregulated in human glomerulonephritis and in a variety of experimental animal models of renal diseases, including glomerulonephritis (7,8), renal ablation (9), and ischemia/reperfusion injury (10). Blocking antibodies against ICAM-1 prevent leukocyte influx into the glomeruli and renal injury in experimental glomerulonephritis (7,8) and renal ablation models (9). We previously (11) demonstrated the accumulation of macrophages and increased expression of cell adhesion molecules, such as ICAM-1 and selectins, in the kidneys of patients with diabetic nephropathy. Furthermore, we reported (12) that the upregulation of ICAM-1 associated with macrophage infiltration occurs in very early stages, soon after the induction of diabetes, and is maintained throughout the observation period in streptozotocin (STZ)-induced diabetic rats. In addition to type 1 diabetic models, glomerular infiltration of macrophages is also seen in models of type 2 diabetes (13,14). We also demonstrated that the administration of anti–ICAM-1 antibody prevents the infiltration of macrophages in diabetic rat

From the Department of Medicine and Clinical Science, Okayama University Graduate School of Medicine and Dentistry, Okayama, Japan.

Address correspondence and reprint requests to Kenichi Shikata, MD, Department of Medicine and Clinical Science, Okayama University Graduate School of Medicine and Dentistry, 2-5-1 Shikata-cho, Okayama 700-8558, Japan. E-mail: shikata@md.okayama-u.ac.jp.

Received for publication 3 December 2002 and accepted in revised form 14 July 2003.

AGE, advanced glycation end product; ECM, extracellular matrix; FITC, fluorescein isothiocyanate; ICAM, intercellular adhesion molecule; mAb, monoclonal antibody; NIH, National Institutes of Health; PAM, periodic acid–methenamine silver; STZ, streptozotocin; TGF, transforming growth factor; VCAM, vascular cell adhesion molecule.

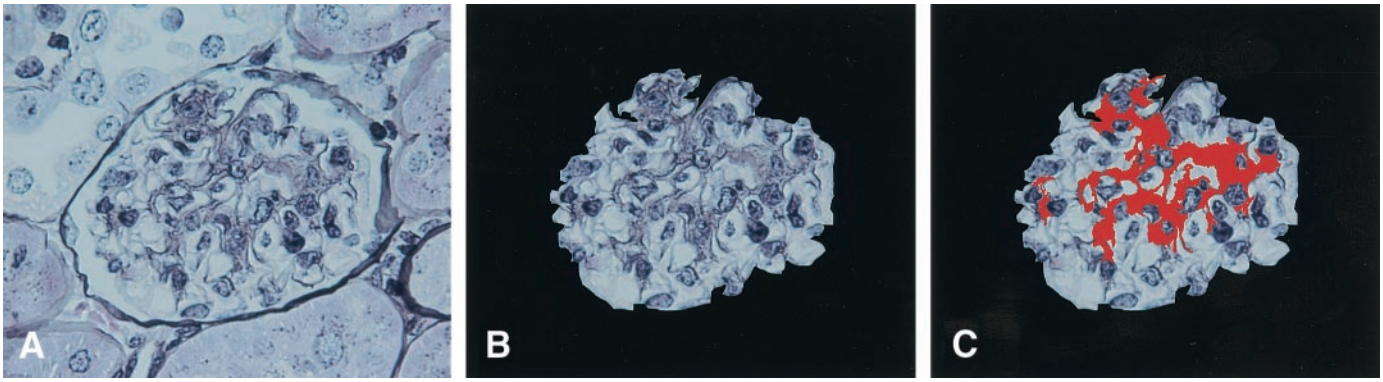

FIG. 1. Morphometric analysis. *A*: PAM staining of a kidney section. Original magnification was ×400. *B*: Glomerular size (tuft area) was measured first by tracing the tuft. *C*: Mesangial matrix area is defined as the PAM-positive area (red area) in the tuft area. The mesangial matrix index represents the ratio of mesangial matrix area divided by tuft area.

glomeruli, indicating that ICAM-1 is a critical molecule for infiltration of macrophages in diabetic nephropathy (12). Chemokines, such as monocyte chemoattractant protein (MCP)-1, are also induced in renal tissues of diabetic patients and diabetic animals (15,16).

The above data suggest the possible involvement of inflammatory processes in the pathogenesis of diabetic nephropathy. Long-term studies are required to examine the histological changes in the kidney of diabetic animals. However, it is difficult to inhibit macrophage infiltration over long periods in such animal models. Because ICAM-1 is a critical molecule for macrophage infiltration into renal tissue, macrophage infiltration should be suppressed in ICAM-1 knockout mice (*ICAM-1*$^{-/-}$ mice) under diabetic conditions. The present study was designed to examine the role of ICAM-1 and macrophages in the pathogenesis of diabetic nephropathy. For this purpose, we induced diabetes in *ICAM-1*$^{-/-}$ mice and wild-type (*ICAM-1*$^{+/+}$) mice and compared the histological and metabolic changes at the end of a 6-month follow-up period after the induction of diabetes.

RESEARCH DESIGN AND METHODS

Animals. *ICAM-1*$^{-/-}$ mice (C57BL/6J background) (17) were purchased from The Jackson Laboratory (Bar Harbor, ME). C57BL/6J mice (*ICAM-1*$^{+/+}$ mice) were used as controls.

Experimental protocol. Male *ICAM-1*$^{+/+}$ and *ICAM-1*$^{-/-}$ mice aged 8 weeks were divided into four groups: *1*) nondiabetic *ICAM-1*$^{+/+}$ mice (n = 10), *2*) nondiabetic *ICAM-1*$^{-/-}$ mice (n = 10), *3*) STZ-induced diabetic *ICAM-1*$^{+/+}$ mice (n = 10), and *4*) diabetic *ICAM-1*$^{-/-}$ mice (n = 10). Mice in the diabetic groups received an intraperitoneal injection of STZ (Sigma Chemical, St. Louis, MO) at 200 mg/kg in citrate buffer (pH 4.5). Nondiabetic *ICAM-1*$^{+/+}$ and *ICAM-1*$^{-/-}$ mice received citrate buffer injections only. All mice had free access to standard diet and tap water. All procedures were performed according to the Guidelines for Animal Experiments at Okayama University Medical School, Japanese Government Animal Protection and Management Law (no. 105), and Japanese Government Notification on Feeding and Safekeeping of Animals (no. 6). Six months after the induction of diabetes, all mice were killed, and the kidneys were harvested. Kidneys were weighed and fixed in 10% formalin for periodic acid–methenamine silver (PAM) and azan staining, and the remaining tissues were embedded in OCT compound (Sakura Finetechnical, Tokyo, Japan) and immediately frozen in acetone cooled on dry ice.

Metabolic data. Blood glucose, urinary creatinine, urinary albumin excretion (24 h), systolic blood pressure, and body weight were measured at 0, 1, 3, and 6 months. Urine collection was performed for 24 h with each mouse individually housed in a metabolic cage with free access to food and water. Serum creatinine was measured at 6 months after the onset of diabetes. Blood glucose was measured by the glucose oxidase method. Creatinine was measured by the enzymatic method. Urinary albumin concentration was measured by nephelometry (Organon Teknika-Cappel, Durham, NC). Blood pressure was measured by the tail-cuff method (Softron). HbA_{1c} was measured at 6 months after induction of diabetes by latex-agglutination assay. Creatinine clearance was calculated in individual mice.

Light microscopy. Renal tissues were fixed in 10% formalin and embedded in paraffin in routine fashion. Tissue sections were cut at 4-μm thickness, dewaxed, and stained with PAM and azan. To evaluate glomerular size, 10 randomly selected glomeruli in the cortex per animal (totaling 100 glomeruli for each group) were examined under high magnification (×400). Glomerular tuft area was measured by manually tracing the glomerular tuft using PhotoShop version 6 (Adobe Systems, San Jose, CA) and analyzed by National Institutes of Health (NIH) Image version 1.6. Mesangial matrix area was defined as the PAM-positive area within the tuft area. The mesangial matrix index represented the ratio of mesangial matrix area divided by the tuft area (Fig. 1). The results are expressed as means ± SE (in micrometers squared).

Tissue preparation for electron microscopy and morphometric analysis of mesangial matrix area. Tissue preparation was performed as previously described (18). Briefly, renal cortical specimens were immersed in 2.5% glutaraldehyde in 0.1 mol/l cacodylate buffer (pH 7.2, 2 h, 4°C), postfixed in 0.1 mol/l osmium tetroxide (2 h, 4°C), and then embedded in Epon following dehydration in a graded series of ethanol preparations. Thin sections were stained with uranyl acetate and lead citrate and examined with an electron microscope (Hitachi H7100) at 100 kV. Glomeruli were photographed at a magnification of ×1,000. Mesangial matrix index was defined as the proportion of the glomerular tuft occupied by the mesangial matrix area (excluding nuclei). Mesangial matrix areas of five glomeruli in each kidney were analyzed. Mesangial matrix areas were selected using PhotoShop and measured with NIH Image.

Immunohistochemical staining. Immunoperoxidase and immunofluorescence staining were performed as previously described (12). Fresh frozen sections were cut at 4-μm thickness using a cryostat. To evaluate infiltration of macrophages, a specific rat monoclonal antibody (mAb) against mouse monocyte/macrophage (F4/80) was applied to the fresh frozen sections as the primary reaction, followed by a second reaction with biotin-labeled goat anti-rat IgG antibody. Finally, the avidin-biotin coupling reaction was performed on the sections using a Vectastain Elite kit (Vector Laboratories, Burlingame, CA). Intraglomerular F4/80-positive cells were counted in 20 glomeruli per animal (totaling 200 glomeruli for each group). The average number per glomerulus was used for the estimation. To evaluate the expression of TGF-β, a rabbit antibody to TGF-β was used as a primary antibody, followed by a second reaction with biotin-labeled donkey anti-rabbit IgG antibody. Ten glomeruli were examined per animal (totaling 100 glomeruli for each group) under high magnification (×400), and the TGF-β–positive area in a glomerulus was measured using NIH Image. The TGF-β–positive area of each glomerulus was expressed relative to the mean value of TGF-β–positive areas in nondiabetic *ICAM-1*$^{+/+}$ mice. To visualize the expression of ICAM-1 and vascular cell adhesion molecule (VCAM)-1, goat anti-mouse ICAM-1 antibody and rat anti-mouse VCAM-1 mAb were used for the primary reactions, and fluorescein isothiocyanate (FITC)-labeled anti-goat IgG antibody and anti-rat IgG antibody were applied to the sections, respectively. To characterize the change in mesangial matrix proteins, rabbit anti–type IV collagen antibody was used for the primary reactions followed by a second reaction with FITC-labeled anti-rabbit IgG. Micrographic fluorescence photos

TABLE 1
Metabolic data

	Nondiabetic mice		Diabetic mice	
	ICAM-1$^{+/+}$	*ICAM-1*$^{-/-}$	*ICAM-1*$^{+/+}$	*ICAM-1*$^{-/-}$
n	10	10	10	10
Systolic blood pressure (mmHg)	96.9 ± 3.9	105.0 ± 1.8	106.0 ± 2.7	100.1 ± 3.9
HbA_{1c} (%)	3.7 ± 0.1	3.7 ± 0.1	9.4 ± 0.5*	9.8 ± 0.2*
Creatinine clearance ($\mu l \cdot min^{-1} \cdot g$ body wt^{-1})	6.5 ± 1.3	5.2 ± 1.6	25.2 ± 3.9*	21.5 ± 2.7*
Body weight (g)	29.1 ± 0.7	31.0 ± 0.7	17.9 ± 0.8*	22.1 ± 1.1*†
Kidney weight (g)	0.31 ± 0.01	0.39 ± 0.01*	0.47 ± 0.01*	0.39 ± 0.02‡§
Relative kidney weight (mg/g body wt)	10.8 ± 0.4	13.1 ± 0.3	26.8 ± 1.3*	19.3 ± 0.8*‖

Data are means ± SE. *$P < 0.0001$ vs. nondiabetic *ICAM-1*$^{+/+}$ mice; †$P < 0.05$ vs. diabetic *ICAM-1*$^{+/+}$ mice; ‡$P < 0.0005$ vs. nondiabetic *ICAM-1*$^{+/+}$ mice; §$P < 0.01$ vs. diabetic *ICAM-1*$^{+/+}$ mice; ‖$P < 0.0001$ vs. diabetic *ICAM-1*$^{+/+}$ mice.

were obtained using a confocal laser fluorescence microscope (LSM-510; Carl Zeiss, Jena, Germany). Quantification of type IV collagen immunofluorescence intensity was performed as follows. Color images were obtained as PICT files from the LSM-510. Image files in PICT format were inverted and opened in gray-scale mode using NIH Image. The type IV collagen expression was calculated using the formula, [x(density) × positive area (in micrometers squared)], where the staining density is indicated by a number from 0 to 255 in gray scale. The type IV collagen expression of each glomerulus was estimated as the ratio to the mean expression in nondiabetic *ICAM-1*$^{+/+}$ mice. Ten glomeruli were examined per animal for type IV collagen expression (totaling 100 glomeruli for each group).

Western blot analysis of type IV collagen in the kidneys.

Sample preparation. Renal cortex was minced by leather blades and put into 1.5-mm^3 Eppendorf tubes, and then Laemmli's sample buffer (containing 30% glycerol, 0.9% SDS, 1 mol/l Tris-HCl, and 15% 2-mercaptoethanol) was added. Tissues in each tube were homogenized by passing through needles from 18 to 26 gauges, 20 times for each needle, in numerical order. The homogenates were then cleared by centrifugation, and the protein concentration of each resulting supernatant was determined using an RC DC protein assay kit (Bio-Rad, Hercules, CA).

Western blotting. Immunoblotting was fundamentally performed as previously described (19). Briefly, samples containing 15 μg protein were boiled for 3 min and then subjected to 12.5% SDS-PAGE. The separated proteins were transferred to polyvinylidene difluoride membranes by electrotransfer. The blots were subsequently blocked with 5% BSA in Tris-buffered saline containing 0.1% Tween-20 at room temperature for 1 h and then incubated at 4°C overnight with 1:100 rabbit anti-human type IV collagen antibody. After washing three times for 10 min with Tris-buffered saline containing 0.1% Tween-20, the membrane was incubated with a 1:1,000 dilution of horseradish peroxidase–linked anti-rabbit IgG secondary antibody at room temperature for 1 h. The blots were then visualized with the enhanced chemiluminescence Western blot detection system (Amersham Biosciences, Amersham Place, U.K.). The primary antibody recognizes the α1-subunit of human type IV collagen and shows a distinct cross-reactivity with mouse type IV collagen. The amount of type IV collagen was analyzed using Image QuaNT analysis software version 4.2-J (Molecular Dynamics, Sunnyvale, CA).

Antibodies. Rat anti-mouse monocyte/macrophage mAb (F4/80) was purchased from Jackson Immunoresearch Laboratories (West Grove, PA). Goat anti-mouse ICAM-1 polyclonal antibody (M-19); rabbit anti-human TGF-β1, -β2, and -β3 rabbit polyclonal antibody (H112); and rabbit anti-human type IV collagen antibody (H234) were purchased from Santa Cruz Biotechnology (Santa Cruz, CA). Rat anti-mouse VCAM-1 mAb was purchased from Endogen (Woburn, MA). Rabbit anti-mouse type IV collagen antibody was purchased from Chemicon International (Temecula, CA). Biotin-labeled goat anti-rat IgG antibody, FITC-labeled donkey anti-goat IgG antibody, biotin-labeled donkey anti-rabbit IgG antibody, and FITC-labeled goat anti-rat IgG antibody were purchased from Jackson Immunoresearch Laboratories.

Statistical analysis. All data are expressed as means ± SE. One-way ANOVA followed by the Scheffe method was used to compare the means of group data. A P value <0.05 denoted the presence of a statistically significant difference.

RESULTS

Metabolic data at the end of the 6-month observation period. At 6 months after induction of diabetes, HbA_{1c} and creatinine clearance in both diabetic *ICAM-1*$^{+/+}$ and *ICAM-1*$^{-/-}$ mice were significantly higher than in nondiabetic *ICAM-1*$^{+/+}$ and *ICAM-1*$^{-/-}$ mice. There was no significant difference in HbA_{1c} and creatinine clearance between diabetic *ICAM-1*$^{+/+}$ and *ICAM-1*$^{-/-}$ mice (Table 1). Body weight was lower in both diabetic *ICAM-1*$^{+/+}$ and *ICAM-1*$^{-/-}$ mice compared with nondiabetic mice. Kidney weights were higher in diabetic *ICAM-1*$^{+/+}$ mice compared with nondiabetic mice. On the other hand, there was no difference in kidney weight between nondiabetic and diabetic *ICAM-1*$^{-/-}$ mice. In addition, kidney weight per body weight was significantly increased in both diabetic groups; however, the ratio was significantly lower in diabetic *ICAM-1*$^{-/-}$ mice compared with diabetic *ICAM-1*$^{+/+}$ mice (Table 1).

Expression of ICAM-1 and VCAM-1 and infiltration of macrophages. ICAM-1 protein expression was prominent in the glomeruli of diabetic *ICAM-1*$^{+/+}$ mice but was undetectable in nondiabetic and diabetic *ICAM-1*$^{-/-}$ mice (Fig. 2*A–D*). The staining with VCAM-1 in the glomeruli was weak in all groups. The differences in glomerular VCAM-1 expression between nondiabetic and diabetic mice and between diabetic *ICAM-1*$^{+/+}$ and *ICAM-1*$^{-/-}$ mice were minimal (data not shown). The number of macrophages in the glomeruli was higher in both diabetic groups at the end of the 6-month follow-up period compared with the respective nondiabetic groups (3.19 ± 0.12 vs. 0.56 ± 0.18 per glomerulus for diabetic vs. nondiabetic *ICAM-1*$^{+/+}$ mice, respectively, $P < 0.0001$; 1.35 ± 0.09 vs. 0.79 ± 0.06 per glomerulus for diabetic vs. nondiabetic *ICAM-1*$^{-/-}$ mice, respectively, $P < 0.0005$) (Fig. 2*E–I*). Infiltration of macrophages into glomeruli was significantly suppressed in diabetic *ICAM-1*$^{-/-}$ mice compared with diabetic *ICAM-1*$^{+/+}$ mice ($P < 0.0001$).

Urinary albumin excretion. As shown in Fig. 3, urinary albumin excretion increased progressively during the study in diabetic mice. However, urinary albumin concentrations in diabetic *ICAM-1*$^{-/-}$ mice were significantly lower than in diabetic *ICAM-1*$^{+/+}$ mice at 3 months (47.3 ± 5.1 vs. 84.6 ± 5.1 μg/day, $P < 0.0001$) and at 6 months (31.4 ± 6.7 vs. 83.6 ± 10.9 μg/day, $P < 0.05$) after the induction of diabetes (Fig. 3).

Light microscopy. Representative glomeruli in PAM-stained sections are shown in Fig. 4*A–D*. Glomerular hypertrophy and mesangial matrix expansion were observed in diabetic *ICAM-1*$^{+/+}$ mice at the end of the 6-month observation period. These changes, however, were not prominent in diabetic *ICAM-1*$^{-/-}$ mice as compared with diabetic *ICAM-1*$^{+/+}$ mice. We also investigated changes

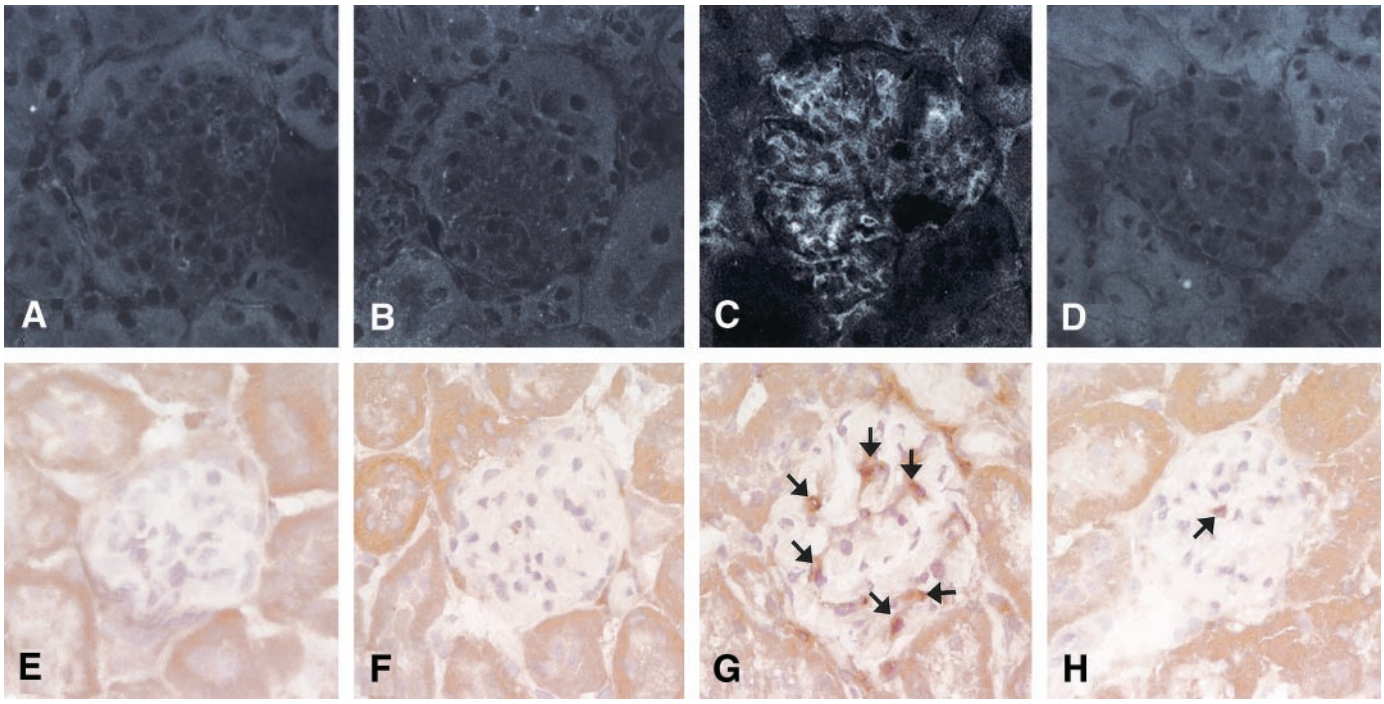

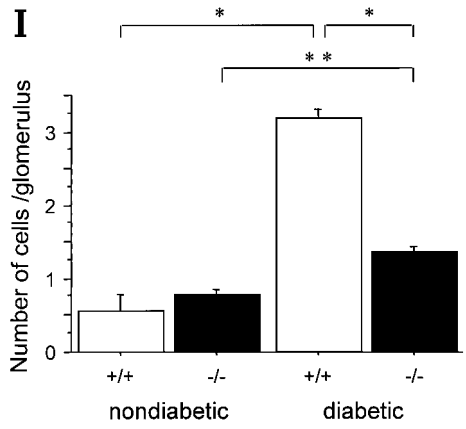

FIG. 2. Expression of ICAM-1 in the glomeruli (*A–D*), macrophage infiltration into the glomeruli (*E–H*), and number of macrophages in the glomeruli (*I*). *A–D*: ICAM-1 expression was increased in the glomeruli of diabetic *ICAM-1*$^{+/+}$ mice (*C*), but not detected in those of diabetic *ICAM-1*$^{-/-}$ mice (*D*). *E–H*: Macrophage (arrows) infiltration into glomeruli was also prominent in diabetic *ICAM-1*$^{+/+}$ mice (*G*), whereas it was minimal in diabetic *ICAM-1*$^{-/-}$ mice (*H*). *A* and *E*: Nondiabetic *ICAM-1*$^{+/+}$ mice. *B* and *F*: Nondiabetic *ICAM-1*$^{-/-}$ mice. *C* and *G*: Diabetic *ICAM-1*$^{+/+}$ mice. *D* and *H*: Diabetic *ICAM-1*$^{-/-}$ mice. Original magnification was ×400. *I*: The quantitative analysis for the number of intraglomerular macrophages. Data are means ± SE. **P* < 0.0001; ***P* < 0.0005; +/+, *ICAM-1*$^{+/+}$ mice; −/−, *ICAM-1*$^{-/-}$ mice.

in the interstitium in azan-stained sections. Interstitial fibrosis was prominent in diabetic *ICAM-1*$^{+/+}$ mice, whereas it was mild in diabetic *ICAM-1*$^{-/-}$ mice as compared with diabetic *ICAM-1*$^{+/+}$ mice (Fig. 4*E–H*). There was no histological change between nondiabetic *ICAM-1*$^{-/-}$ and *ICAM-1*$^{+/+}$ mice. Both glomerular area and mesangial matrix index were increased in diabetic *ICAM-1*$^{+/+}$ mice. These values were significantly lower in diabetic *ICAM-1*$^{-/-}$ mice (tuft area, 3,829 ± 83 vs. 4,370 ± 137 μm^2, $P < 0.005$; mesangial matrix index, 5.6 ± 0.4 vs. 7.6 ± 0.6%, $P < 0.01$) (Fig. 4*I* and *J*).

Electron microscopy. Representative electron microscopic photos are shown in Fig. 5. Mesangial matrix index was significantly increased in diabetic groups (8.18 ± 0.63 vs. 18.1 ± 1.34% for nondiabetic vs. diabetic *ICAM-1*$^{+/+}$ mice, respectively, $P < 0.0001$; 6.64 ± 0.60 vs. 10.5 ± 0.82% for nondiabetic vs. diabetic *ICAM-1*$^{-/-}$ mice, respectively, $P = 0.022$). However, the index was significantly lower in diabetic *ICAM-1*$^{-/-}$ mice compared with diabetic *ICAM-1*$^{+/+}$ mice ($P < 0.0001$).

Expression of TGF-β and type IV collagens. TGF-β–positive areas in glomeruli were larger in diabetic mice compared with nondiabetic mice. Furthermore, the TGF-β–positive area in diabetic *ICAM-1*$^{-/-}$ mice was lower than in diabetic *ICAM-1*$^{+/+}$ mice (212 ± 20 vs. 316 ± 21% of nondiabetic *ICAM-1*$^{+/+}$ mice, $P < 0.0005$) (Fig. 6*A–D* and *I*). The intensity of type IV collagen in glomeruli was higher in diabetic mice compared with nondiabetic mice,

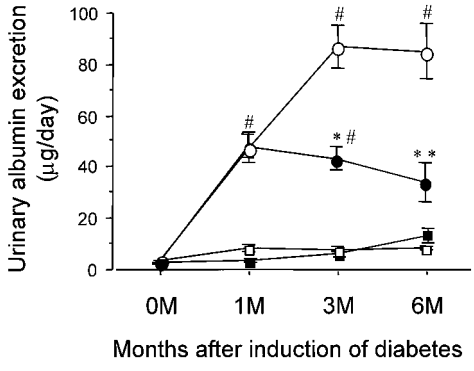

FIG. 3. Time course of changes in urinary albumin excretion. Urinary albumin excretion increased progressively in diabetic *ICAM-1*$^{+/+}$ mice (○) during the 6-month observation period following induction of diabetes. In diabetic *ICAM-1*$^{-/-}$ mice (●), urinary albumin excretion increased initially but reached a plateau at 3 months after induction of diabetes and then decreased compared with *ICAM-1*$^{+/+}$ mice. No changes were noted in nondiabetic mice of both groups. Data are means ± SE. □, nondiabetic *ICAM-1*$^{+/+}$ mice; ■, nondiabetic *ICAM-1*$^{-/-}$ mice. **P* < 0.0001; ***P* < 0.05 vs. diabetic *ICAM-1*$^{+/+}$ mice; #*P* < 0.0001 vs. nondiabetic *ICAM-1*$^{+/+}$ mice.

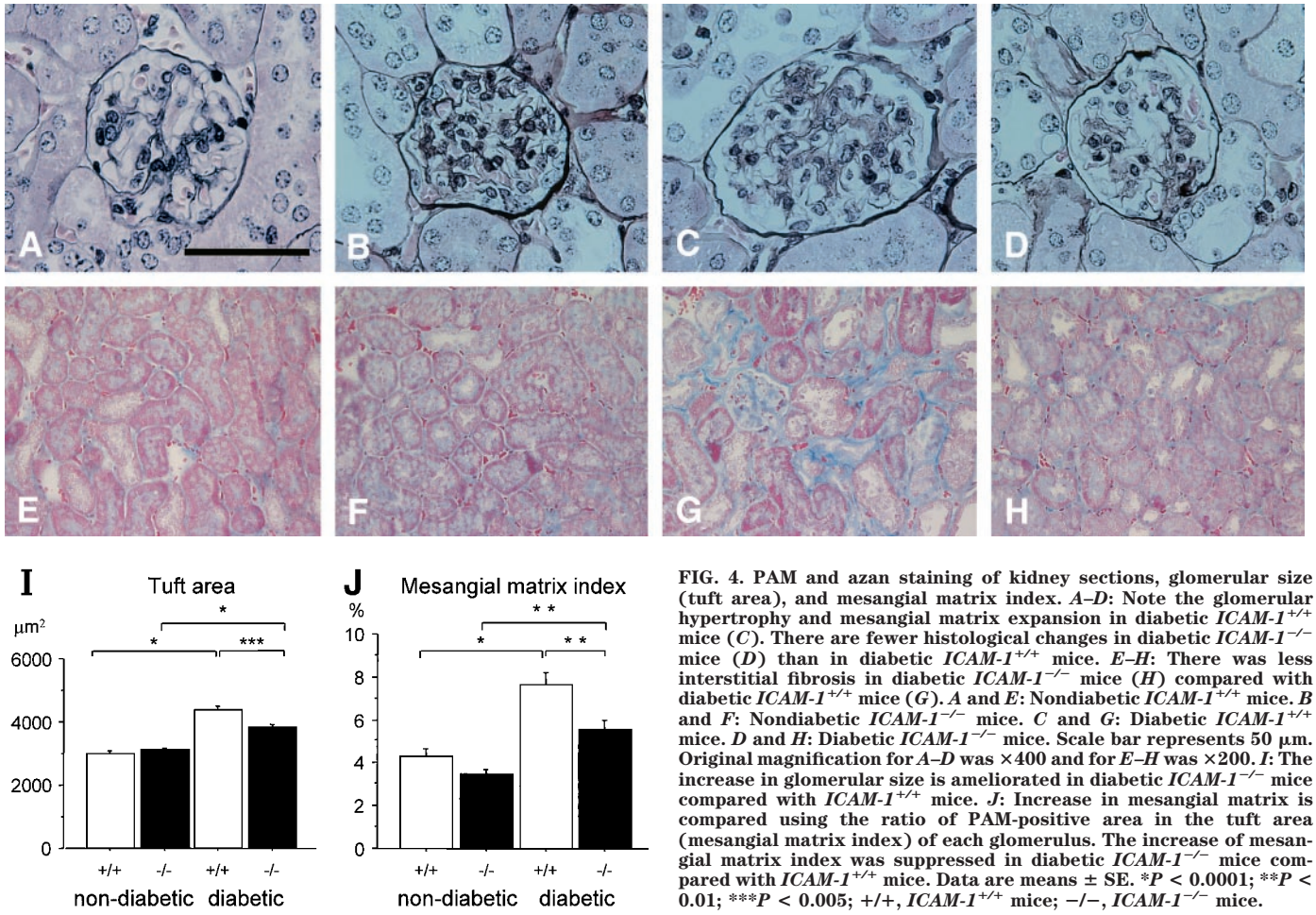

FIG. 4. PAM and azan staining of kidney sections, glomerular size (tuft area), and mesangial matrix index. *A–D*: Note the glomerular hypertrophy and mesangial matrix expansion in diabetic *ICAM-1*$^{+/+}$ mice (*C*). There are fewer histological changes in diabetic *ICAM-1*$^{-/-}$ mice (*D*) than in diabetic *ICAM-1*$^{+/+}$ mice. *E–H*: There was less interstitial fibrosis in diabetic *ICAM-1*$^{-/-}$ mice (*H*) compared with diabetic *ICAM-1*$^{+/+}$ mice (*G*). *A* and *E*: Nondiabetic *ICAM-1*$^{+/+}$ mice. *B* and *F*: Nondiabetic *ICAM-1*$^{-/-}$ mice. *C* and *G*: Diabetic *ICAM-1*$^{+/+}$ mice. *D* and *H*: Diabetic *ICAM-1*$^{-/-}$ mice. Scale bar represents 50 μm. Original magnification for *A–D* was ×400 and for *E–H* was ×200. *I*: The increase in glomerular size is ameliorated in diabetic *ICAM-1*$^{-/-}$ mice compared with *ICAM-1*$^{+/+}$ mice. *J*: Increase in mesangial matrix is compared using the ratio of PAM-positive area in the tuft area (mesangial matrix index) of each glomerulus. The increase of mesangial matrix index was suppressed in diabetic *ICAM-1*$^{-/-}$ mice compared with *ICAM-1*$^{+/+}$ mice. Data are means ± SE. **P* < 0.0001; ***P* < 0.01; ****P* < 0.005; +/+, *ICAM-1*$^{+/+}$ mice; −/−, *ICAM-1*$^{-/-}$ mice.

and the intensity in diabetic *ICAM-1*$^{-/-}$ mice was lower than in diabetic *ICAM-1*$^{+/+}$ mice (111 ± 2 vs. 147 ± 3% of nondiabetic *ICAM-1*$^{+/+}$ mice, $P < 0.0001$) (Fig. 6*E–H*, and *J*).

Western blot analysis of type IV collagen protein expression levels in the kidneys. As shown in Fig. 7, Western blot analysis revealed increased type IV collagen protein expression in the kidneys of diabetic *ICAM-1*$^{+/+}$ mice, whereas the type IV collagen expression was significantly suppressed in diabetic *ICAM-1*$^{-/-}$ mice compared with diabetic *ICAM-1*$^{+/+}$ mice (73 ± 17 vs. 236 ± 62% for diabetic *ICAM-1*$^{-/-}$ and diabetic *ICAM-1*$^{+/+}$ mice, respectively, $P = 0.048$).

DISCUSSION

We induced diabetes in *ICAM-1*$^{-/-}$ and *ICAM-1*$^{+/+}$ mice and compared the progression of renal injury associated with hyperglycemia in the present study. Diabetic *ICAM-1*$^{+/+}$ mice (C57BL/6 mice) developed mild diabetic nephropathy as previously described (20). Our results showed that glomerular infiltration of macrophages, renal and glomerular hypertrophy, overproduction of TGF-β, accumulation of type IV collagen in glomeruli, and albuminuria were significantly suppressed in *ICAM-1*$^{-/-}$ mice when compared with *ICAM-1*$^{+/+}$ mice at 6 months after induction of diabetes.

The phenotypes of *ICAM-1*$^{-/-}$ mice used in this study were originally reported by Sligh et al. (17). *ICAM-1*$^{-/-}$ mice are fertile and show no apparent developmental defects. Their immune responses are impaired, i.e., their neutrophil emigration in response to chemical peritonitis and decreased contact hypersensitivity is impaired, and with the exception of an increased level of circulating neutrophils and a slight increase in body weight, no obvious abnormal phenotype is seen in normal conditions (21,22). Under normal conditions, no obvious abnormalities in histology and function of the kidneys are observed in these mice. However, ICAM-1 is a critical molecule for leukocyte infiltration in inflammatory processes, and amelioration of experimentally induced autoimmune glomerulonephritis was noted in *ICAM-1*$^{-/-}$ mice, which was associated with reduced glomerular leukocyte infiltration (23,24).

ICAM-1 was upregulated in glomeruli of diabetic *ICAM-1*$^{+/+}$ mice. Although it is still controversial whether hyperglycemia per se can induce the expression of ICAM-1 on vascular endothelial cells, recent studies have suggested several possible mechanisms of ICAM-1 induction in diabetic renal tissues. *1*) ICAM-1 is induced by inflammatory cytokines such as tumor necrosis factor-α, interleukin-1, and interferon-γ (25). *2*) Activation of protein kinase C results in upregulation of ICAM-1 on endothelial cells (26). *3*) AGEs enhance the expression of cell adhesion molecules, including ICAM-1 on vascular endothelial cells (27,28). *4*) Shear stress could also stimulate the induction of ICAM-1 (29). We previously reported (9,12) that shear stress,

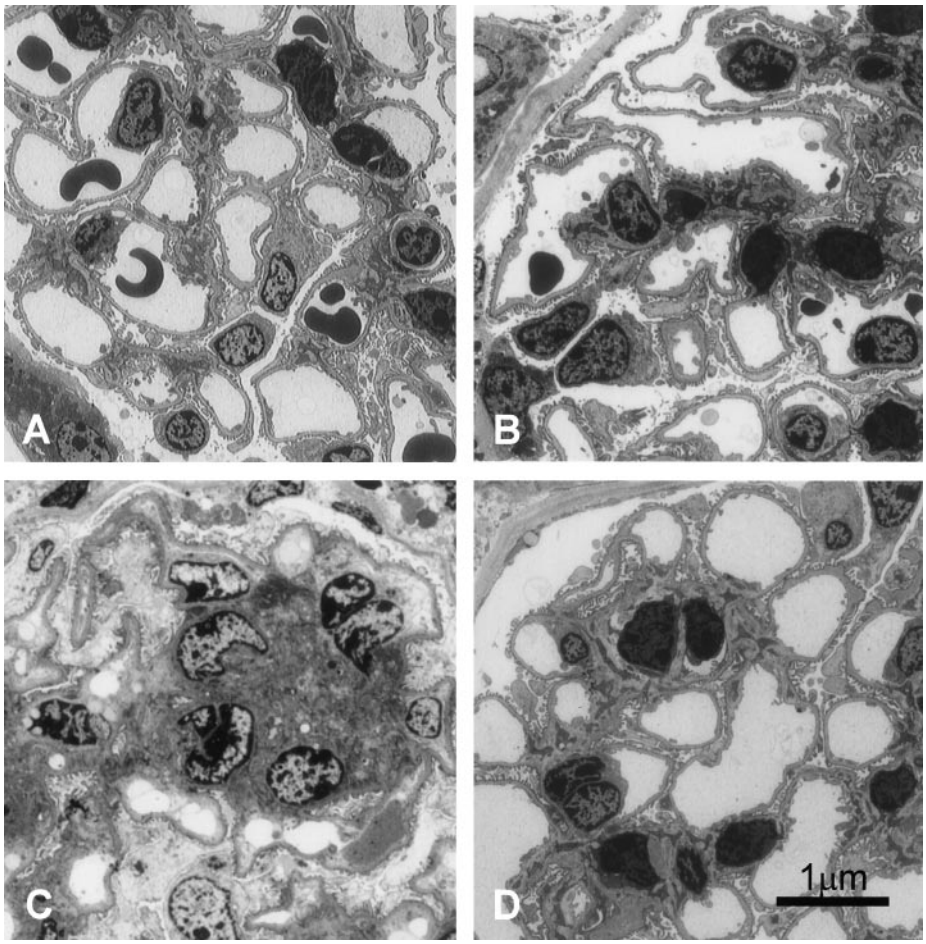

FIG. 5. Electron microscopic photos of kidney sections. Expansion of the mesangial matrix is prominent in diabetic *ICAM-1*$^{+/+}$ mice (*C*) and not apparent in diabetic *ICAM-1*$^{-/-}$ mice (*D*). *A*: Nondiabetic *ICAM-1*$^{+/+}$ mice. *B*: Nondiabetic *ICAM-1*$^{-/-}$ mice. *C*: Diabetic *ICAM-1*$^{+/+}$ mice. *D*: Diabetic *ICAM-1*$^{-/-}$ mice. Scale bar represents 1 μm. Original magnification was ×1,000.

which is increased by hyperfiltration of glomerular endothelial cells, is one of the mediators of ICAM-1 induction in glomeruli. *5*) Oxidative stress has been documented to increase ICAM-1 expression (30). *6*) Osmotic agents upregulate ICAM-1 expression in rat mesangial cells (31) and in human umbilical vein endothelial cells (32).

Our results showed that the infiltration of macrophages into the glomeruli was lower in diabetic *ICAM-1*$^{-/-}$ mice compared with diabetic *ICAM-1*$^{+/+}$ mice (reduction rate 78.5%), suggesting that ICAM-1 is a critical molecule for the infiltration of macrophages into glomeruli in diabetic nephropathy. This finding is consistent with our previous study (12), using anti–ICAM-1 antibody in STZ-induced diabetic rats.

Several adhesion molecules are involved in leukocyte infiltration in inflammatory lesions. VCAM-1, in addition to ICAM-1, is a major adhesion molecule. We examined the expression of VCAM-1 in this study, but VCAM-1 expression in glomeruli was low, and little difference was seen between diabetic *ICAM-1*$^{-/-}$ and *ICAM-1*$^{+/+}$ mice. Although we could not detect a compensatory upregulation of VCAM-1, it may be possible that VCAM-1 is involved, at least in part, in macrophage infiltration in diabetic *ICAM-1*$^{-/-}$ mice.

Glomerular hypertrophy associated with increased mesangial matrix proteins mainly composed of type IV collagens is a characteristic feature of diabetic nephropathy (33). In this regard, TGF-β is thought to play a central role in the enhancement of glomerular extracellular matrix production in diabetic nephropathy (34,35). Albuminuria is the most established marker of glomerular injury in the early stages of diabetic nephropathy. Increased mesangial matrix, glomerular hypertrophy, and albuminuria were significantly suppressed in diabetic *ICAM-1*$^{-/-}$ mice compared with diabetic *ICAM-1*$^{+/+}$ mice. Expression levels of TGF-β and type IV collagen were also lower in diabetic *ICAM-1*$^{-/-}$ mice compared with diabetic *ICAM-1*$^{+/+}$ mice. These results suggest that ICAM-1–dependent infiltration of macrophages plays a critical role in the development of diabetic glomerulosclerosis. There was no significant difference in urinary albumin excretion between diabetic *ICAM-1*$^{+/+}$ mice and diabetic *ICAM-1*$^{-/-}$ mice at 1 month after induction of diabetes, suggesting that ICAM-1 is not involved in increased albuminuria in the very early stages of diabetic nephropathy. A possible explanation is that albuminuria is related to a rapid increase in urine volume and changes in glomerular hemodynamics over the month after induction of diabetes in this study.

Macrophages produce various types of cytokines (which stimulate cell proliferation) and ECM, and they induce tissue injury. Recent studies have reported that the depletion of leukocytes by irradiation decreased the gene expression of TGF-β and type IV collagen in the glomeruli of diabetic rats at 4 weeks after induction of diabetes, suggesting the pathological role of macrophages in the increased expression of ECM proteins (36). ECMs that include type IV collagen are produced by mesangial cells. With respect to the interaction between macrophages and

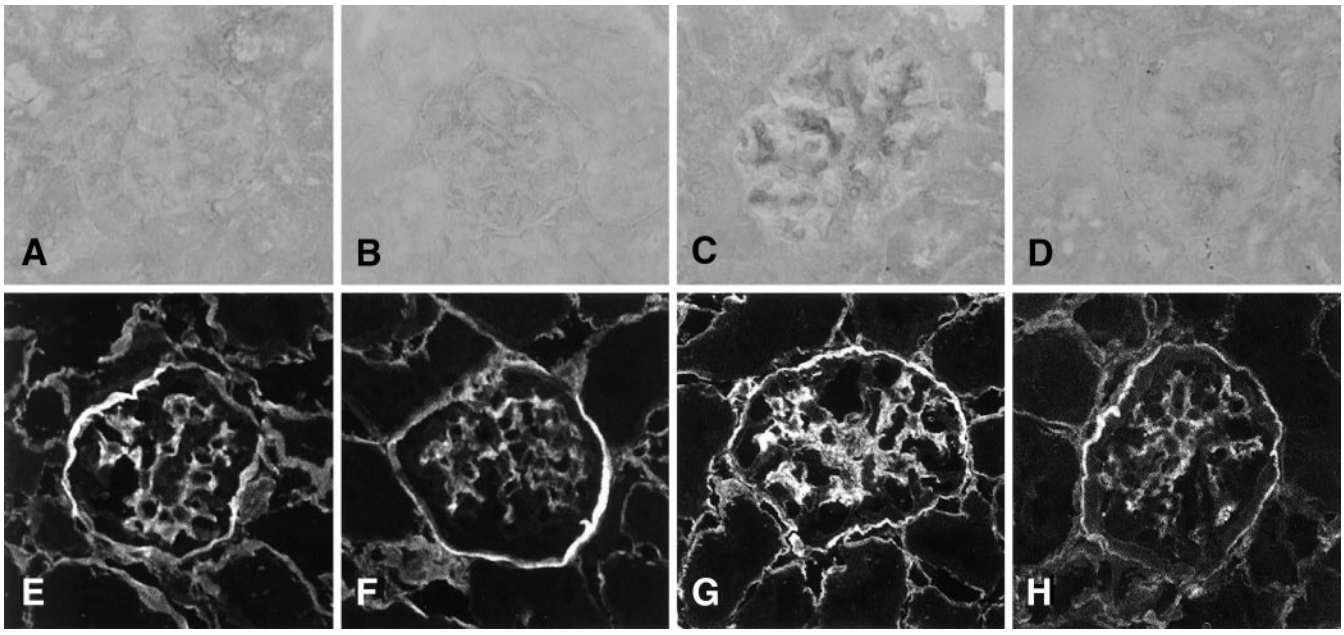

FIG. 6. Histological expression and quantitative analysis of TGF-β and type IV collagen in the glomeruli of kidney sections. TGF-β expression was evaluated by immunohistochemistry. TGF-β was prominent in the glomeruli of diabetic *ICAM-1*$^{+/+}$ mice (*C*) compared with diabetic *ICAM-1*$^{-/-}$ mice (*D*). The TGF-β–positive area in each glomeruli is expressed here relative to the mean value of TGF-β–positive areas in nondiabetic *ICAM-1*$^{+/+}$ mice (*I*). Expression of type IV collagen, which is estimated by fluorescence intensity, was also increased in the glomeruli of both diabetic groups (*G* and *H*), although the increase was smaller in diabetic *ICAM-1*$^{-/-}$ mice (*H* and *J*). *A* and *E*: Nondiabetic *ICAM-1*$^{+/+}$ mice. *B* and *F*: Nondiabetic *ICAM-1*$^{-/-}$ mice. *C* and *G*: Diabetic *ICAM-1*$^{+/+}$ mice. *D* and *H*: Diabetic *ICAM-1*$^{-/-}$ mice. Magnification is ×400. Data are means ± SE. **P* < 0.0001; ***P* < 0.0005; +/+, *ICAM-1*$^{+/+}$ mice; −/−, *ICAM-1*$^{-/-}$ mice.

mesangial cells, Pawluczyk and Harris (37) reported that the culture supernatant of macrophages stimulates mesangial cells to produce fibronectin in vitro. When considering the above findings with the present results, we can speculate that infiltrated glomerular macrophages stimulate mesangial cells to secrete TGF-β through certain cytokines. TGF-β can in turn induce ECM overproduction from mesangial cells in autocrine and paracrine fashions. On the other hand, previous studies (38) have indicated that macrophages themselves can induce TGF-β. Thus, macrophages could secrete TGF-β, which stimulates mesangial cells to produce ECM proteins in diabetic glomeruli.

Interstitial fibrosis is another important histopathological change that correlates with renal function in diabetic nephropathy (39). ICAM-1 is expressed in peritubular capillaries and tubular epithelial cells in *ICAM-1*$^{+/+}$ mice, whereas the density of macrophages in the interstitium and interstitial fibrosis was minimal in diabetic *ICAM-1*$^{-/-}$ mice in the present study, suggesting that ICAM-1 plays a major role in interstitial infiltration of macrophages and subsequent interstitial fibrosis.

In conclusion, we have demonstrated that renal and glomerular hypertrophy, mesangial matrix expansion, and albuminuria were ameliorated in diabetic *ICAM-1*$^{-/-}$ mice compared with *ICAM-1*$^{+/+}$ mice. These results suggest that ICAM-1 plays a critical role in the progression of diabetic nephropathy.

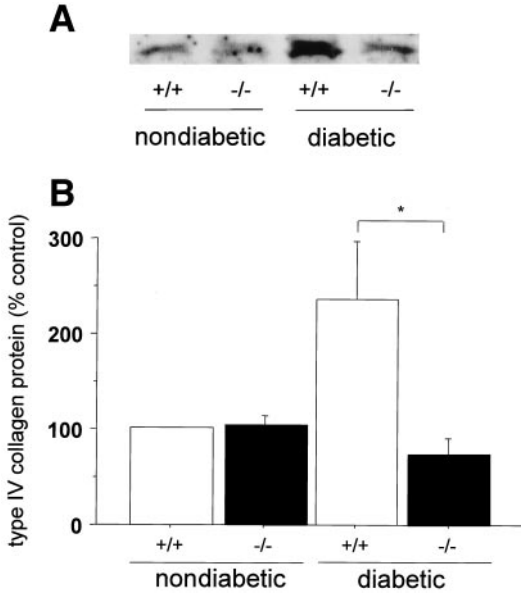

FIG. 7. Western blot analysis of type IV collagen in the kidneys. Kidneys were homogenized and type IV collagen was analyzed by Western blotting. *A*: Representative bands of type IV collagen are presented. *B*: Type IV collagen protein level was increased in diabetic *ICAM-1*$^{+/+}$ mice but was significantly lower in diabetic *ICAM-1*$^{-/-}$ mice than in diabetic *ICAM-1*$^{+/+}$ mice. **P* < 0.05 vs. diabetic *ICAM-1*$^{+/+}$ mice.

ACKNOWLEDGMENTS

This study was supported in part by a Grant-in-Aid for Scientific Research (C11671036 and C13671116 to K.S. and 12770582 to M.M.) from the Ministry of Education, Science, Culture, Sports, and Technology of Japan.

We thank Atsuko Yuasa (Okayama Central Hospital, Okayama, Japan) and Toshiyo Hashimoto (Okayama University Graduate School) for excellent technical assistance.

REFERENCES

1. Koya D, Jirousek MR, Lin YW, Ishii H, Kuboki K, King GL: Characterization of protein kinase C beta isoform activation on the gene expression of transforming growth factor-beta, extracellular matrix components, and prostanoids in the glomeruli of diabetic rats. *J Clin Invest* 100:115–126, 1997
2. Yang CW, Vlassara H, Peten EP, He CJ, Striker GE, Striker LJ: Advanced glycation end products up-regulate gene expression found in diabetic glomerular disease. *Proc Natl Acad Sci U S A* 91:9436–9440, 1994
3. Pugliese G, Pricci F, Romeo G, Pugliese F, Mene P, Giannini S, Cresci B, Galli G, Rotella CM, Vlassara H, Di Mario U: Upregulation of mesangial growth factor and extracellular matrix synthesis by advanced glycation end products via a receptor-mediated mechanism. *Diabetes* 46:1881–1887, 1997
4. Furuta T, Saito T, Ootaka T, Soma J, Obara K, Abe K, Yoshinaga K: The role of macrophages in diabetic glomerulosclerosis. *Am J Kidney Dis* 21:480–485, 1993
5. Shikata K, Makino H: Role of macrophages in the pathogenesis of diabetic nephropathy. *Contrib Nephrol* 134:46–54, 2001
6. Staunton DE, Marlin SD, Stratowa C, Dustin ML, Springer TA: Primary structure of ICAM-1 demonstrates interaction between members of the immunoglobulin and integrin supergene families. *Cell* 52:925–933, 1988
7. Kawasaki K, Yaoita E, Yamamoto T, Tamatani T, Miyasaka M, Kihara I: Antibodies against intercellular adhesion molecule-1 and lymphocyte function-associated antigen-1 prevent glomerular injury in rat experimental crescentic glomerulonephritis. *J Immunol* 150:1074–1083, 1993
8. Wada J, Shikata K, Makino H, Morioka S, Hirata K, Ota K, Tamatani T, Miyasaka M, Horiuchi T, Noji S, Nishikawa K, Myokai F, Taniguchi S, Kanwar Y, Ota Z: The critical role of intercellular adhesion molecule-1 in Masugi nephritis in rats. *Nephron* 73:264–272, 1996
9. Miyatake N, Shikata K, Sugimoto H, Kushiro M, Shikata Y, Ogawa S, Hayashi Y, Miyasaka M, Makino H: Intercellular adhesion molecule 1 mediates mononuclear cell infiltration into rat glomeruli after renal ablation. *Nephron* 79:91–98, 1998
10. Kelly KJ, Williams WW Jr, Colvin RB, Meehan SM, Springer TA, Gutierrez-Ramos JC, Bonventre JV: Intercellular adhesion molecule-1-deficient mice are protected against ischemic renal injury. *J Clin Invest* 97:1056–1063, 1996
11. Hirata K, Shikata K, Matsuda M, Akiyama K, Sugimoto H, Kushiro M, Makino H: Increased expression of selectins in kidneys of patients with diabetic nephropathy. *Diabetologia* 41:185–192, 1998
12. Sugimoto H, Shikata K, Hirata K, Akiyama K, Matsuda M, Kushiro M, Shikata Y, Miyatake N, Miyasaka M, Makino H: Increased expression of intercellular adhesion molecule-1 (ICAM-1) in diabetic rat glomeruli: glomerular hyperfiltration is a potential mechanism of ICAM-1 upregulation. *Diabetes* 46:2075–2081, 1997
13. Coimbra TM, Janssen U, Grone HJ, Ostendorf T, Kunter U, Schmidt H, Brabant G, Floege J: Early events leading to renal injury in obese Zucker (fatty) rats with type II diabetes. *Kidney Int* 57:167–182, 2000
14. Lavaud S, Michel O, Sassy-Prigent C, Heudes D, Bazin R, Bariety J, Chevalier J: Early influx of glomerular macrophages precedes glomerulosclerosis in the obese Zucker rat model. *J Am Soc Nephrol* 7:2604–2615, 1996
15. Kato S, Luyckx VA, Ots M, Lee KW, Ziai F, Troy JL, Brenner BM, MacKenzie HS: Renin-angiotensin blockade lowers MCP-1 expression in diabetic rats. *Kidney Int* 56:1037–1048, 1999
16. Wada T, Furuichi K, Sakai N, Iwata Y, Yoshimoto K, Shimizu M, Takeda SI, Takasawa K, Yoshimura M, Kida H, Kobayashi KI, Mukaida N, Naito T, Matsushima K, Yokoyama H: Up-regulation of monocyte chemoattractant protein-1 in tubulointerstitial lesions of human diabetic nephropathy. *Kidney Int* 58:1492–1499, 2000
17. Sligh JE Jr, Ballantyne CM, Rich SS, Hawkins HK, Smith CW, Bradley A, Beaudet AL: Inflammatory and immune responses are impaired in mice deficient in intercellular adhesion molecule 1. *Proc Natl Acad Sci U S A* 90:8529–8533, 1993
18. Makino H, Shikata K, Hironaka K, Kushiro M, Yamasaki Y, Sugimoto H, Ota Z, Araki N, Horiuchi S: Ultrastructure of nonenzymatically glycated mesangial matrix in diabetic nephropathy. *Kidney Int* 48:517–526, 1995
19. Shikata Y, Shikata K, Matsuda M, Sugimoto H, Wada J, Makino H: Signaling transduction pathway of angiotensin II in human mesangial cells: mediation of focal adhesion and GTPase activating proteins. *Biochem Biophys Res Commun* 257:234–238, 1999
20. Zheng F, Striker GE, Esposito C, Lupia E, Striker LJ: Strain differences rather than hyperglycemia determine the severity of glomerulosclerosis in mice. *Kidney Int* 54:1999–2007, 1998
21. Collins RG, Velji R, Guevara NV, Hicks MJ, Chan L, Beaudet AL: P-selectin or intercellular adhesion molecule (ICAM)-1 deficiency substantially protects against atherosclerosis in apolipoprotein E-deficient mice. *J Exp Med* 191:189–194, 2000
22. Dong ZM, Gutierrez-Ramos JC, Coxon A, Mayadas TN, Wagner DD: A new class of obesity genes encodes leukocyte adhesion receptors. *Proc Natl Acad Sci U S A* 94:7526–7530, 1997
23. Janssen U, Ostendorf T, Gaertner S, Eitner F, Hedrich HJ, Assmann KJ, Floege J: Improved survival and amelioration of nephrotoxic nephritis in intercellular adhesion molecule-1 knockout mice. *J Am Soc Nephrol* 9:1805–1814, 1998
24. Bullard DC, King PD, Hicks MJ, Dupont B, Beaudet AL, Elkon KB: Intercellular adhesion molecule-1 deficiency protects MRL/MpJ-Fas(lpr) mice from early lethality. *J Immunol* 159:2058–2067, 1997
25. Wertheimer SJ, Myers CL, Wallace RW, Parks TP: Intercellular adhesion molecule-1 gene expression in human endothelial cells: differential regulation by tumor necrosis factor-alpha and phorbol myristate acetate. *J Biol Chem* 267:12030–12035, 1992
26. Lane TA, Lamkin GE, Wancewicz E: Modulation of endothelial cell expression of intercellular adhesion molecule 1 by protein kinase C activation. *Biochem Biophys Res Commun* 161:945–952, 1989
27. Vlassara H, Fuh H, Donnelly T, Cybulsky M: Advanced glycation end products promote adhesion molecule (VCAM-1, ICAM-1) expression and atheroma formation in normal rabbits. *Mol Med* 1:447–456, 1995
28. Sengoelge G, Fodinger M, Skoupy S, Ferrara I, Zangerle C, Rogy M, Horl WH, Sunder-Plassmann G, Menzel J: Endothelial cell adhesion molecule and PMNL response to inflammatory stimuli and AGE-modified fibronectin. *Kidney Int* 54:1637–1651, 1998
29. Nagel T, Resnick N, Atkinson WJ, Dewey CF Jr, Gimbrone MA Jr: Shear stress selectively upregulates intercellular adhesion molecule-1 expression in cultured human vascular endothelial cells. *J Clin Invest* 94:885–891, 1994
30. Lo SK, Janakidevi K, Lai L, Malik AB: Hydrogen peroxide-induced increase in endothelial adhesiveness is dependent on ICAM-1 activation. *Am J Physiol* 264:L406–L412, 1993
31. Park CW, Kim JH, Lee JH, Kim YS, Ahn HJ, Shin YS, Kim SY, Choi EJ, Chang YS, Bang BK, Lee JW: High glucose-induced intercellular adhesion molecule-1 (ICAM-1) expression through an osmotic effect in rat mesangial cells is PKC-NF-kappa B-dependent. *Diabetologia* 43:1544–1553, 2000
32. Taki H, Kashiwagi A, Tanaka Y, Horiike K: Expression of intercellular adhesion molecules 1 (ICAM-1) via an osmotic effect in human umbilical vein endothelial cells exposed to high glucose medium. *Life Sci* 58:1713–1721, 1996
33. Adler S: Structure-function relationships associated with extracellular matrix alterations in diabetic glomerulopathy. *J Am Soc Nephrol* 5:1165–1172, 1994
34. Ziyadeh FN, Hoffman BB, Han DC, Iglesias-De La Cruz MC, Hong SW, Isono M, Chen S, McGowan TA, Sharma K: Long-term prevention of renal insufficiency, excess matrix gene expression, and glomerular mesangial matrix expansion by treatment with monoclonal antitransforming growth factor-beta antibody in db/db diabetic mice. *Proc Natl Acad Sci U S A* 97:8015–8020, 2000
35. Sharma K, Ziyadeh FN: Hyperglycemia and diabetic kidney disease: the case for transforming growth factor-β as a key mediator. *Diabetes* 44: 1139–1146, 1995
36. Sassy-Prigent C, Heudes D, Mandet C, Belair MF, Michel O, Perdereau B, Bariety J, Bruneval P: Early glomerular macrophage recruitment in streptozotocin-induced diabetic rats. *Diabetes* 49:466–475, 2000
37. Pawluczyk IZ, Harris KP: Macrophages promote prosclerotic responses in cultured rat mesangial cells: a mechanism for the initiation of glomerulosclerosis. *J Am Soc Nephrol* 8:1525–1536, 1997
38. Leonarduzzi G, Scavazza A, Biasi F, Chiarpotto E, Camandola S, Vogel S, Dargel R, Poli G: The lipid peroxidation end product 4-hydroxy-2,3-nonenal up-regulates transforming growth factor beta1 expression in the macrophage lineage: a link between oxidative injury and fibrosclerosis. *Faseb J* 11:851–857, 1997
39. Mauer SM, Steffes MW, Ellis EN, Sutherland DE, Brown DM, Goetz FC: Structural-functional relationships in diabetic nephropathy. *J Clin Invest* 74:1143–1155, 1984